

## Compressive-stress-induced $T_c$ increase of the low- $T_c$ $\text{Bi}_{1.6}\text{Pb}_{0.4}\text{Sr}_2\text{Ca}_2\text{Cu}_3\text{O}_x$ phase

Yoshitake Nishi, Kazuya Oguri, Hideo Ohinata, Kenji Tanioka,  
Yuichiro Kita, and Nobuyuki Ninomiya

*Department of Materials Science, Tokai University, Kitakaname, Hiratsuka, Kanagawa, Japan*

(Received 19 October 1989)

The effect of compressive stress on  $T_c$  is studied for the low- $T_c$   $\text{Bi}_{1.6}\text{Pb}_{0.4}\text{Sr}_2\text{Ca}_2\text{Cu}_3\text{O}_x$  phase. Although stress decreases the  $T_c$  of the high- $T_c$  sample, the small compressive stress increases the  $T_c$  of the low- $T_c$  phase. The maximum  $T_c^{\text{off}}$  is about 113.6 K at 0.01 mA/mm<sup>2</sup> (current density) and 3.92 N/mm<sup>2</sup> of the low- $T_c$  phase where  $T_c^{\text{off}}$  is 96.2 K before loading. The maximum  $T_c^{\text{off}}$  is larger than the unloaded value (109.3 K) of the high- $T_c$   $\text{Bi}_{1.6}\text{Pb}_{0.4}\text{Sr}_2\text{Ca}_2\text{Cu}_3\text{O}_x$  sample. Based on the results of x-ray-diffraction, electrical-resistivity, and Seebeck-effect measurements, the  $T_c$  is dominated by carrier concentration and crystal perfection of the lattice ordering.

### I. INTRODUCTION

From an engineering point of view, it is important to know the effect of compressive stress on  $T_c$ . Effects of compressive stress on  $T_c$  have been reported for  $\text{YBa}_2\text{Cu}_3\text{O}_{7-y}$ .<sup>1,2</sup> Although the compressive stress increased  $T_c^{\text{on}}$  and  $T_c^{\text{mid}}$ , the remarkable  $T_c^{\text{off}}$  increase with pressure had never been reported. However, we have recently found the small compressive-stress-induced  $T_c^{\text{off}}$  to increase for  $\text{YBa}_2\text{Cu}_3\text{O}_{7-y}$ .<sup>3,4</sup> Thus, we undertake to obtain information of the influence of the stress on  $T_c$  for the low- ( $T_c=96$  K) and high- ( $T_c=109$  K)  $T_c$   $\text{Bi}_{1.6}\text{Pb}_{0.4}\text{Sr}_2\text{Ca}_2\text{Cu}_3\text{O}_x$  samples.

### II. EXPERIMENTAL PROCEDURE

Samples with nominal composition were prepared by high-purity powders of CuO (99.9 mass%), PbO (99.9 mass%), SrCO<sub>3</sub> (99.9 mass%), CaCO<sub>3</sub> (99.9 mass%), and Bi<sub>2</sub>O<sub>3</sub> (99.99 mass%). The powders were mixed and sintered in air at 1023 K for 8 h and then air cooled. After crushing, the sintered powders were resintered in air at 1073 K for 18 h and then air cooled. After crushing, a pellet-shaped tablet, 2 mm thick and 13 mm in diameter, was sintered in air at 1123 K for 12 h (low- $T_c$  sample) and 75 h (high- $T_c$  sample) and then furnace cooled.

The compressive stress was provided by a mechanical tester.<sup>4</sup> The electrical resistivity (Refs. 4 and 5) and Seebeck effect (Refs. 6 and 7) were measured in the tester. The stress was loaded by the stainless-steel rod attached to the specimen on the copper block. The electrical resistivity was measured using a standard four-probe technique and a Keithley 181 nanovoltmeter. The temperature was measured by an Au-Fe-chromel thermocouple attached to the specimen in a cryostat at equilibrium temperatures.<sup>4</sup> The structure of the samples was tetragonal.<sup>5</sup>

### III. RESULTS AND DISCUSSION

#### A. $T_c$ measurement

Figure 1 shows the temperature dependence of electrical resistivity ( $R$ ) of the unloaded and loaded (3.92

N/mm<sup>2</sup>)  $\text{Bi}_{1.6}\text{Pb}_{0.4}\text{Sr}_2\text{Ca}_2\text{Cu}_3\text{O}_x$ . The lower the temperature, the lower the electrical resistivity becomes. Offset  $T_c^{\text{off}}$  and onset  $T_c^{\text{on}}$  of the transition are defined as the temperatures corresponding to the achievement of zero resistivity (below  $10^{-9}$  Ω m at 1 mA/mm<sup>2</sup> of the current density) and to the deviation of the electrical resistivity. The deviated point is taken at  $d(R/R_{300\text{K}})/dT=0.004$ , where  $d(R/R_{300\text{K}})/dT$  and  $R_{300\text{K}}$  are the slope of the reduced electrical resistivity ( $R/R_{300\text{K}}$ ) against the temperature graph and the resistivity at 300 K, respectively. The midpoint is designated as  $T_c^{\text{mid}}$ .

Figures 2 and 3 show changes in  $T_c^{\text{off}}$ ,  $T_c^{\text{mid}}$ , and  $T_c^{\text{on}}$  with compressive stress. The solid and dashed lines are for the low- and high- $T_c$  samples, respectively. The small stress enhances  $T_c^{\text{off}}$ ,  $T_c^{\text{mid}}$ , and  $T_c^{\text{on}}$  of the low- $T_c$  phase (solid lines), although the values decrease in the high- $T_c$  sample (dashed lines). The slope of  $T_c^{\text{on}}$  is larger than that of  $T_c^{\text{off}}$  below the maximum value of the solid lines;  $T_c$  decreases above the maximum value. The maximum values of  $T_c^{\text{off}}$ ,  $T_c^{\text{mid}}$ , and  $T_c^{\text{on}}$  are found at 3.92 N/mm<sup>2</sup> (solid lines). The maximum  $T_c^{\text{off}}$  is about 113.6 K at 0.01 mA/mm<sup>2</sup> of the current density for the low- $T_c$  phase which  $T_c^{\text{off}}$  is 96.2 K before the loading. The maximum value is larger than the unloaded value (109.3 K) of the high- $T_c$   $\text{Bi}_{1.6}\text{Pb}_{0.4}\text{Sr}_2\text{Ca}_2\text{Cu}_3\text{O}_x$  sample.

#### B. X-ray diffraction

Figure 4 shows x-ray-diffraction peaks of the (002) plane for the low- and high- $T_c$   $\text{Bi}_{1.6}\text{Pb}_{0.4}\text{Sr}_2\text{Ca}_2\text{Cu}_3\text{O}_x$  samples. The low- $T_c$  (96.2 K) sample shows at 5.9° of the (002) peak angle and shows that the double CuO layer appears.<sup>8</sup> On the other hand, the high- $T_c$  sample has two (002) peaks at 5.9° and 4.8° (Ref. 9). The high- $T_c$  phase (above 100 K) often has the triple CuO layer, which peak is found at 4.8°. Thus, the high- $T_c$  sample is a mixture of the high- $T_c$  and low- $T_c$  phases.

Figures 5 and 6 show the changes in the lattice constant ( $c$ ) and full width at half maximum intensity (FWHM) against the compressive stress of the unloaded  $\text{Bi}_{1.6}\text{Pb}_{0.4}\text{Sr}_2\text{Ca}_2\text{Cu}_3\text{O}_x$  samples after the loading. The solid line is for the low- $T_c$  phase. The dashed lines are

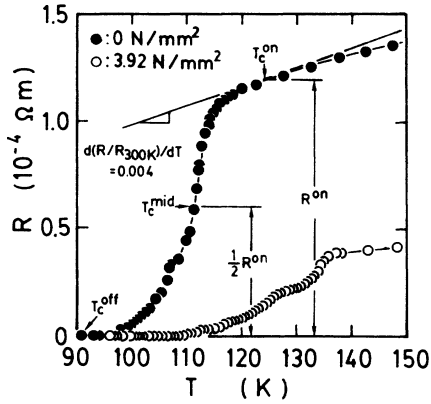


FIG. 1. Changes in electrical resistivity ( $R$ ) vs temperature ( $T$ ) for unloaded ( $\bullet$ ) and loaded ( $3.92 \text{ N/mm}^2$ ) ( $\circ$ )  $\text{Bi}_{1.6}\text{Pb}_{0.4}\text{Sr}_2\text{Ca}_2\text{Cu}_3\text{O}_x$ .

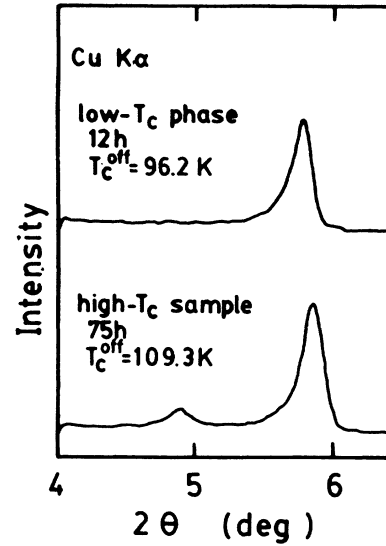


FIG. 4. X-ray diffraction pattern of the (002) plane for low- and high- $T_c$   $\text{Bi}_{1.6}\text{Pb}_{0.4}\text{Sr}_2\text{Ca}_2\text{Cu}_3\text{O}_x$  samples.

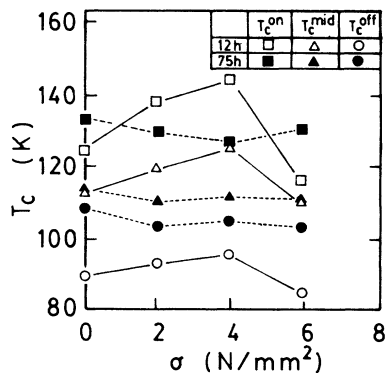


FIG. 2. Changes in the superconducting transition temperature ( $T_c$ ) with compressive stress ( $\sigma$ ) for the  $\text{Bi}_{1.6}\text{Pb}_{0.4}\text{Sr}_2\text{Ca}_2\text{Cu}_3\text{O}_x$  phases at  $1 \text{ mA/mm}^2$  of current density.

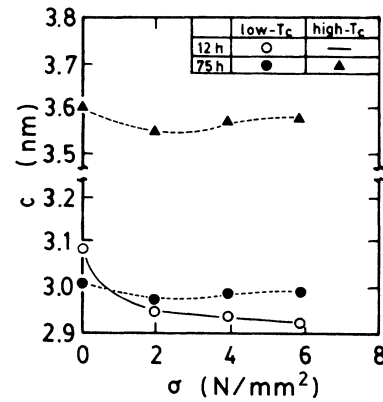


FIG. 5. Changes in the lattice constant ( $c$ ) against compressive stress ( $\sigma$ ) of unloaded  $\text{Bi}_{1.6}\text{Pb}_{0.4}\text{Sr}_2\text{Ca}_2\text{Cu}_3\text{O}_x$  samples after loading.

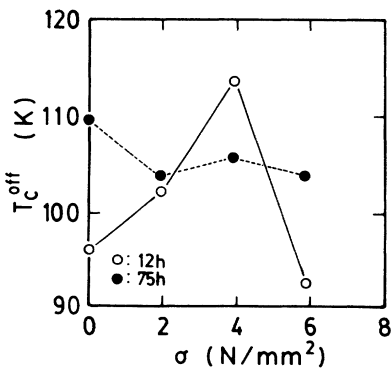


FIG. 3. Changes in the offset temperature ( $T_c^{\text{off}}$ ) of the superconducting transition temperature with compressive stress ( $\sigma$ ) at  $0.01 \text{ mA/mm}^2$  of current density for the  $\text{Bi}_{1.6}\text{Pb}_{0.4}\text{Sr}_2\text{Ca}_2\text{Cu}_3\text{O}_x$  phases.

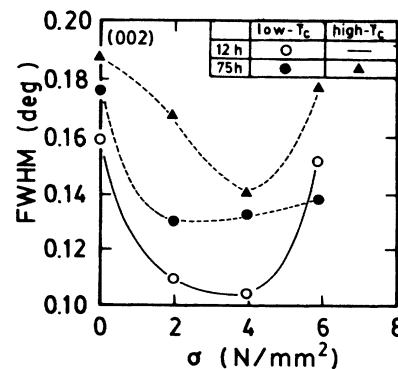


FIG. 6. Changes in FWHM against the compressive stress ( $\sigma$ ) of unloaded  $\text{Bi}_{1.6}\text{Pb}_{0.4}\text{Sr}_2\text{Ca}_2\text{Cu}_3\text{O}_x$  samples after loading.

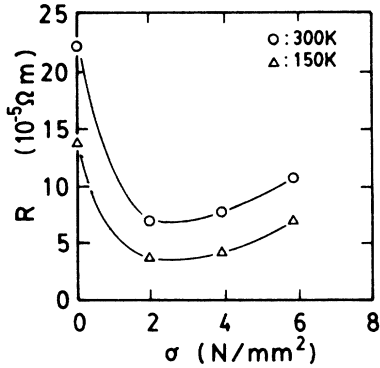


FIG. 7. Changes in electrical resistivity ( $R$ ) against compressive stress ( $\sigma$ ) for the low- $T_c$   $\text{Bi}_{1.6}\text{Pb}_{0.4}\text{Sr}_2\text{Ca}_2\text{Cu}_3\text{O}_x$  phases.

for the high- $T_c$  sample. The small load decreases the lattice constant for 1.96 N/mm<sup>2</sup> of the unloaded sample after the loading (see Fig. 5). The small load decreases FWHM for 3.92 N/mm<sup>2</sup> (see Fig. 6). FWHM is the width of the x-ray-diffraction peaks at half height. Thus, the small compressive stress enhances the crystal perfection of the lattice ordering. These results mean that the small stress easily moves the atoms distributed in expansive (uncompressive) sites, whereas the stress does not easily move the atoms in the compressive sites. Namely, the stress decreases the lattice constant and FWHM. The smaller the FWHM, the higher the degree of the crystal-lattice ordering becomes, resulting in high  $T_c$  by the small amount of the stress in the low- $T_c$  phase.

The excess stress increases FWHM and slightly decreases the lattice constant. They show that the large stress moves the atoms in the compressive stress and disorders the crystal-lattice ordering. Although the similar changes in  $c$  and FWHM are found for the high- $T_c$  samples (dashed lines in Fig. 6), the  $T_c$  increase has never been observed. The slight increases in the lattice constants are found above the minimum point (see dashed lines in Fig. 5). It shows that some disaccommodations (such as microcracks) exist. If the more careful treatment is performed without any disaccommodation, the stress-induced  $T_c$  increase will probably be found in the high- $T_c$   $\text{Bi}_{1.6}\text{Pb}_{0.4}\text{Sr}_2\text{Ca}_2\text{Cu}_3\text{O}_x$  samples.

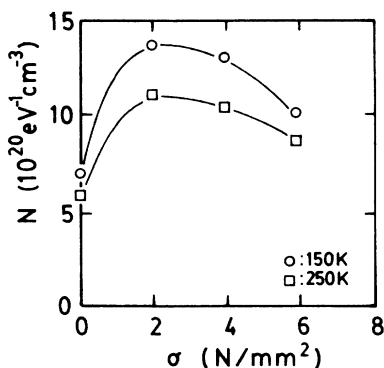


FIG. 8. Changes in density of state ( $N$ ) against compressive stress ( $\sigma$ ) for the low- $T_c$   $\text{Bi}_{1.6}\text{Pb}_{0.4}\text{Sr}_2\text{Ca}_2\text{Cu}_3\text{O}_x$  phases.

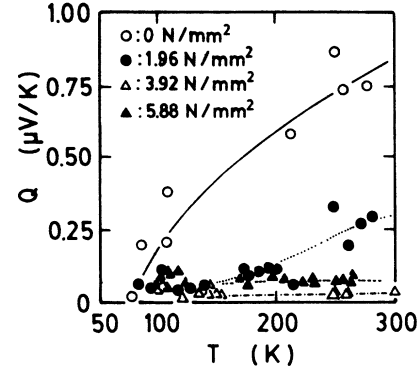


FIG. 9. Changes in the Seebeck coefficient ( $Q$ ) against temperature ( $T$ ) for the low- $T_c$   $\text{Bi}_{1.6}\text{Pb}_{0.4}\text{Sr}_2\text{Ca}_2\text{Cu}_3\text{O}_x$  phases (loaded and unloaded).

### C. Electronic discussion

Carrier concentration ( $c^*$ ) is one of the dominant factors that control the  $T_c$ . The Seebeck constant ( $Q$ ) is expressed by the following.<sup>6,7</sup>

$$Q = \pm(k/e)[\ln(N/c^*) + A]. \quad (1)$$

Here,  $k$ ,  $e$ , and  $N$  are the Boltzmann constant, electron charge, and density of state, respectively;  $A$  is a constant. Thus,  $c^*$  is expressed by the following:

$$c^* = N/\exp[(\pm eQ/k) - A]. \quad (2)$$

To obtain  $c^*$ , the density of state ( $N$ ) is calculated by the use of the electrical resistivity ( $R_e$ ).  $N$  is expressed by the following:<sup>10</sup>

$$N = A'/R_e^{1/2}. \quad (3)$$

Here,  $A'$  is a constant that is dominated by the electron mass, charge, Planck constant, and mean free path. If the stress does not largely change their values, the  $N$  value is inversely proportional to the  $R_e^{1/2}$  value.

Figure 7 shows the change in the electrical resistivity against the stress. The small compressive stress decreases the resistivity and increases the density (see Fig. 8). Here,

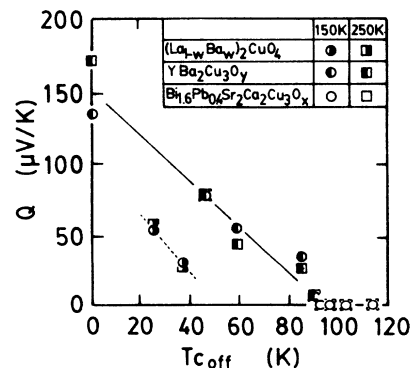


FIG. 10. Changes in the Seebeck coefficient ( $Q$ ) against the offset temperature ( $T_c^{\text{off}}$ ) of the superconducting transition for  $(\text{La}_{1-w}\text{Ba}_w)_2\text{CuO}_4$  (Refs. 12 and 13) and  $\text{YBa}_2\text{Cu}_3\text{O}_y$  (Refs. 13 and 14), together with the unloaded and loaded  $\text{Bi}_{1.6}\text{Pb}_{0.4}\text{Sr}_2\text{Ca}_2\text{Cu}_3\text{O}_x$  phases (see Fig. 9).

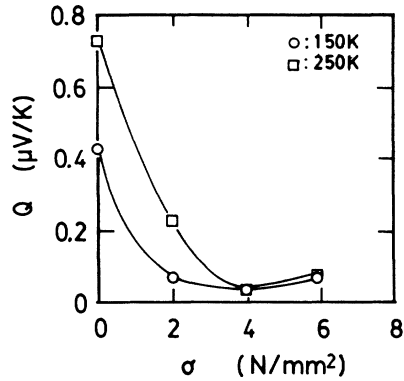


FIG. 11. Changes in the Seebeck coefficient ( $Q$ ) against compressive stress ( $\sigma$ ) for the low- $T_c$   $\text{Bi}_{1.6}\text{Pb}_{0.4}\text{Sr}_2\text{Ca}_2\text{Cu}_3\text{O}_x$  phases.

the electron mean free path is assumed to be constant and to be equal to the lattice constant of the  $c$  axis. Namely, the larger the stress, the higher the density of state becomes, resulting in high  $T_c$ . On the other hand, since the excess stress slightly decreases the density, it decreases the  $T_c$ .

Figure 9 shows the temperature dependence of the Seebeck coefficient ( $Q$ ) for the low- $T_c$   $\text{Bi}_{1.6}\text{Pb}_{0.4}\text{Sr}_2\text{Ca}_2\text{Cu}_3\text{O}_x$  phases that are loaded and unloaded. As compared with the unloaded sample, the loaded samples under the small stress show the temperature-independent Seebeck coefficient. The temperature-independent  $Q$  is considered to be strongly correlated with the electron system.<sup>11,12</sup> If the correlation among electrons is very strong, the Mott-Hubbard band must be formed and the half-filled conduction band is split into two bands.

Based on Eq. (2), the smaller the  $Q$ , the higher the carrier concentration ( $c^*$ ) becomes. Figure 10 shows the relationship between  $Q$  (Ref. 13) and  $T_c^{\text{off}}$  (Refs. 12 and 14) for  $\text{YBa}_2\text{Cu}_3\text{O}_{7-y}$  and  $(\text{La}_{1-w}\text{Ba}_w)_2\text{CuO}_4$ , together with the loaded  $\text{Bi}_{1.6}\text{Pb}_{0.4}\text{Sr}_2\text{Ca}_2\text{Cu}_3\text{O}_x$  phases. The lower the  $Q$ , the higher the  $T_c^{\text{off}}$  becomes for the high- $T_c$  oxides. The  $\text{Bi}_{1.6}\text{Pb}_{0.4}\text{Sr}_2\text{Ca}_2\text{Cu}_3\text{O}_x$  phases show the small  $Q$ . Figure 11 shows change in the  $Q$  against the compressive stress. The small stress decreases  $Q$  rapidly. The excess stress slightly increases  $Q$ . Thus, the  $Q$  change in Fig. 11 coincides with the  $T_c$  change in Figs. 2 and 3.

Since the small stress decreases  $Q$  and increases  $N$ , the

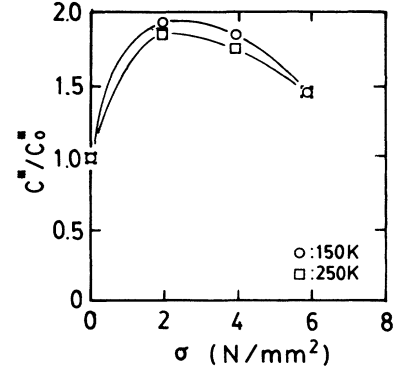


FIG. 12. Changes in reduced carrier concentration ( $C^*/C_0^*$ ) against compressive stress ( $\sigma$ ) for the low- $T_c$   $\text{Bi}_{1.6}\text{Pb}_{0.4}\text{Sr}_2\text{Ca}_2\text{Cu}_3\text{O}_x$  phases.  $C^*$  is the carrier concentration at different loads.  $C_0^*$  is for the unloaded sample.

large value of  $c^*$  is obtained by the small compressive stress by use of Eq. (2). Figure 12 shows the  $c^*$  change against the compressive stress. The  $c^*$  change approximately agrees with the  $T_c$  change (see Figs. 2 and 3). Namely, the higher the carrier concentration, the higher the  $T_c$  becomes for the loaded  $\text{Bi}_{1.6}\text{Pb}_{0.4}\text{Sr}_2\text{Ca}_2\text{Cu}_3\text{O}_x$  phases.

Since the band gaps for the high- $T_c$  oxides are smaller than those of the semiconductors,  $A$  is about zero. Furthermore, the high- $T_c$  oxides show small  $Q$ . The exponential term in Eq. (2) is about 1. Thus, we suggest that  $c^*$  is mainly dominated by the density of state ( $N$ ) for the high- $T_c$  oxides.

#### IV. CONCLUSION

The effect of compressive stress on  $T_c$  is studied for the low- $T_c$   $\text{Bi}_{1.6}\text{Pb}_{0.4}\text{Sr}_2\text{Ca}_2\text{Cu}_3\text{O}_x$  phase. Although the stress decreases  $T_c$  of the high- $T_c$  sample, the small compressive stress increases  $T_c$  of the low- $T_c$  phase. The maximum  $T_c^{\text{off}}$  is about 113.6 K at 3.92 N/mm<sup>2</sup> of the low- $T_c$  phase ( $T_c^{\text{off}}=96.2$  K before the loading). It is larger than the unloaded value (109.3 K) of the high- $T_c$   $\text{Bi}_{1.6}\text{Pb}_{0.4}\text{Sr}_2\text{Ca}_2\text{Cu}_3\text{O}_x$  sample. Based on the results of the x-ray diffraction, electrical resistivity, and Seebeck effect, we conclude that the high carrier concentration and the crystal perfection of the lattice ordering enhance the  $T_c$  value.

<sup>1</sup>M. K. Wu, J. R. Ashburn, and C. T. Torng, Phys. Rev. Lett. **58**, 908 (1987).

<sup>2</sup>S. Yomo, C. Murayama, W. Utsumi, H. Takahashi, T. Yagi, N. Mori, T. Tamegai, A. Watanabe, and Y. Iye, Jpn. J. Appl. Phys. Suppl. **26**, 1107 (1987).

<sup>3</sup>Y. Nishi, N. Ninomiya, and S. Tokunaga, J. Mater. Sci. Lett. **7**, 361 (1988).

<sup>4</sup>Y. Nishi, N. Ninomiya, K. Oguri, and S. Tokunaga, J. Appl. Phys. **65**, 3927 (1989).

<sup>5</sup>Y. Nishi, A. Igarashi, S. Moriya, Y. Kita, and S. Tokunaga, J. Mater. Sci. Lett. **8**, 700 (1989).

<sup>6</sup>N. M. Tallan and I. Bransky, J. Electrochem. Soc. **118**, 345 (1971).

<sup>7</sup>R. F. Brebrick, in *Defects in Solids*, Vol. 2 of *Treatise on Solid*

*State Chemistry*, edited by N. B. Hannay (Plenum, New York, 1975), pp. 357–362.

<sup>8</sup>H. Nobumasa, K. Shimizu, Y. Kitano, and T. Kawai, Jpn. J. Appl. Phys. **27**, L846 (1988).

<sup>9</sup>H. Nobumasa, K. Shimizu, Y. Kitano, and T. Kawai, Jpn. J. Appl. Phys. **27**, L1669 (1988).

<sup>10</sup>N. F. Mott, Philos. Mag. **19**, 835 (1969).

<sup>11</sup>P. M. Chainkin and G. Beni, Phys. Rev. B **13**, 647 (1976).

<sup>12</sup>S. Uchida, Physica B **148**, 185 (1987).

<sup>13</sup>H. Ishii, H. Sato, N. Kanazawa, H. Takagi, S. Uchida, K. Kitazawa, K. Kishio, K. Fueki, and S. Tanaka, Physica B **148**, 419 (1987).

<sup>14</sup>E. Takayama-Muromachi, Y. Uchida, M. Ishii, T. Tanaka, and K. Kato, Jpn. J. Appl. Phys. **26**, L1156 (1987).